

Available online at www.sciencedirect.com

ScienceDirect

journal homepage: www.elsevier.com/locate/radcr

Case Report

Right aortic arch with mirror image branching pattern and isolated left brachiocephalic artery: A case report [☆]

Ayman Nada, MD, PhD*, Joseph P. Cousins, PhD, MD, Humera Ahsan, MD, Jeffrey R. Kunin, MD

Department of Radiology, University of Missouri, One Hospital Dr. Columbia, MO, 65212, USA

ARTICLE INFO

Article history:

Received 6 July 2020

Revised 11 July 2020

Accepted 11 July 2020

Keywords:

Aortic arch anomalies

Right aortic arch

Isolated left brachiocephalic artery

Mirror-image branching

Nonmirror image branching

CT

ABSTRACT

We present a very rare case of right aortic arch with an isolated left brachiocephalic artery in a 35-year-old female. This entity is an extremely uncommon aortic arch anomaly which has associated multisystem symptoms. We briefly discuss the hypothetical double aortic arch model originally described by Edwards. The aortic embryology can explain the anatomic findings and imaging manifestations of the isolated left brachiocephalic artery. Multimodality imaging evaluation can be helpful in detection and categorization of aortic arch abnormalities. A diagnostic imaging approach should focus on elucidating the abnormal aortic arch and great vessels arrangement with determination of associated cardiac, vascular or visceral congenital abnormalities.

Published by Elsevier Inc. on behalf of University of Washington.

This is an open access article under the CC BY-NC-ND license.

(<http://creativecommons.org/licenses/by-nc-nd/4.0/>)

Introduction

Right-sided aortic arch with an isolated left brachiocephalic artery (ILBA) is an extremely uncommon developmental anomaly in which the left brachiocephalic artery (LBCA) is not connected to the aortic arch [1]. The result of this “isolation” is that the blood supply to the LBCA must arise from collateral vessels and/or a patent ductus arteriosus [2]. The hypothetical double aortic arch model (Fig. 1) described by Edwards can explain the origin of this vascular

anomaly where the arch is interrupted at 2 locations [3].

An ILBA results in numerous clinical manifestations, and in general are referred to as the 3 Hs: head, heart and hand, affecting the central nervous system, cardiopulmonary system and, left upper extremity [1]. The central nervous system manifestations are attributed to vertebrobasilar insufficiency, while cardiopulmonary problems result from pulmonary circulation disturbances which lead to congestive heart failure. Left upper extremity claudication and numbness are the consequences of decreased blood flow to the left subclavian artery (LSA) [1].

[☆] Conflicts of interest: The authors declare no financial or other conflicts of interest.

* Corresponding author.

E-mail address: anada@health.missouri.edu (A. Nada).

<https://doi.org/10.1016/j.radcr.2020.07.027>

1930-0433/Published by Elsevier Inc. on behalf of University of Washington. This is an open access article under the CC BY-NC-ND license. (<http://creativecommons.org/licenses/by-nc-nd/4.0/>)

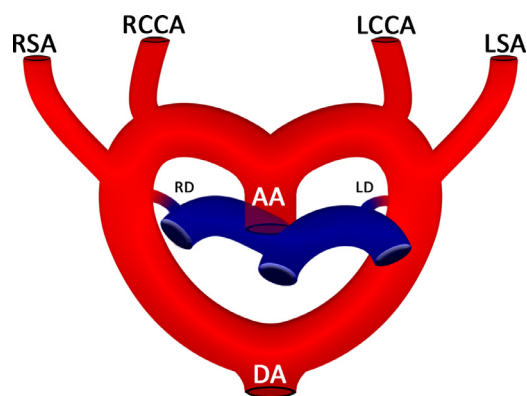


Fig. 1 – Graphic illustration of double aortic arch model of Edwards.

Case report

A 35-year-old female presented with a recent diagnosis of hypertension. The patient had a family history of systemic hypertension. The patient denied any history or current symptoms of stroke, transient ischemic attack symptoms, specifically, neither focal arm or leg weakness, slurred speech, and nor facial droop. The patient had no prior history of smoking. The patient's physical examination was normal apart from a right carotid bruit. Renal and carotid ultrasound duplex were obtained as initial workup for hypertension and observed right carotid bruit. The renal ultrasound was negative for renal artery stenosis or renal parenchymal abnormalities. Carotid ultrasound duplex revealed elevated velocities in the right internal carotid artery of 210/78 cm/s and tardus parvus waveforms throughout the left carotid artery. The left vertebral artery showed tardus parvus and a high resistance waveform with retrograde flow. Further evaluation with a CT angiography (CTA) of the head and neck was obtained. The CTA revealed an abnormal branching pattern of the aortic arch and its great vessels. Findings included a right sided aortic arch with an ILBA (Fig. 2). The origin of left BCA is interrupted from aorta for 3.8 cm (wide arrows in Figs. 2a, c, and d and 3a). The most anterior branch or the first branch arises from the aorta is the right common carotid artery (RCCA). The second branch vessel from the aorta is the right subclavian artery (RSA). The right vertebral artery, which is dominant and hypertrophied, arises from RSA. A moderate sized vessel arises from the left posteromedial wall of the aortic arch (wide black outlined arrow in Fig. 2b and arrow heads in Fig. 2c and d) inferiorly and from the left side which ascends superiorly as a single mediastinal collateral artery (arrows in Fig. 3b, d, e), and provides many collaterals at the left lower neck. The collateral artery gives off branches to supply the nondominant and hypoplastic left vertebral artery at the lower neck (arrow in Fig. 3c). A hypertrophied left paraspinal artery (short white arrows in Fig. 2 c and d) communicates with left posterior auricular artery, a branch from left external carotid artery. Left external carotid artery branches fill from the hypoplastic left common carotid artery (LCCA) which is diminutive in size through the

Table 1 – Demonstrates resultant aortic branching pattern based on regressed segment(s).

Regression of segment(s)	Resultant branching pattern
4	LARCH (normal branching)
5	LARCH with aberrant RSA
4 + 5	LARCH with isolated RSA
6	LARCH with aberrant RBCA
4 + 6	LARCH with isolated RBCA
5 + 6	LARCH with isolated RCCA and aberrant RSA
3	RARCH with mirror image branching
2	RARCH with aberrant LSA
2 + 3	RARCH with isolated LSA
1	RARCH with aberrant LBCA
1 + 3	RARCH with isolated left LBCA
1 + 2	RARCH with isolated LCCA and aberrant LSA
NONE	Double aortic arch

AA, ascending aorta; DA, descending aorta; LCCA, left common carotid artery; LSA, left subclavian artery; LD, left ductus arteriosus; RD, right ductus arteriosus; RCCA, right common carotid artery; RSA, right subclavian artery; LARCH, left aortic arch; RARCH, right aortic arch; RBCA, right brachiocephalic artery; LBCA, left brachiocephalic artery.

supraclavicular segment. This resulted in 2-point collateralization with the left vertebral and external carotid arteries.

Discussion

Normal aortic arch development requires an accurate and stepwise remodeling of the various pharyngeal arch arteries that involve elongation, sprouting/splitting, and regression [4–6]. Cardiac neural crest cells, which are subset of neural crest cells, contribute to outflow tracts septation, and development of ventricular septum, cardiac valves, and pharyngeal arch arteries [5]. The correct development of aortic arch and pulmonary arteries depends significantly on cardiac neural crest cells signaling [7].

The incidence of aortic arch anomalies is approximately 0.5%-3% with approximately 0.05%-0.1% of them as right aortic arch anomaly [8,9]. The most common presentation (approximately 60%) is the "mirror-image type," with a right-sided arch and a LBCA, RCCA, and RSA [9]. The "mirror-image type" is strongly associated with other cardiac anomalies [8]. The next most common presentation (approximately 40%) is a right-sided aortic arch with an aberrant left subclavian artery (ALSA); this mimics the aberrant RSA pattern, with the LCCA arises first, followed by the RCCA, RSA, and then ALSA [9].

Patients with a right aortic arch may be symptomatic or asymptomatic [9]. Symptoms may arise directly from airway or esophageal compression, or indirectly from associated abnormalities including cardiac defects and vascular steals [9].

Most aortic arch abnormalities can be explained by the hypothetical double aortic arch originally proposed by Edwards in 1948 [2]. The aortic arch and great vessels develop from 6 pairs of primitive aortic arches (Table 1 and Fig. 4) which arise and degenerate at different times of embryogen-

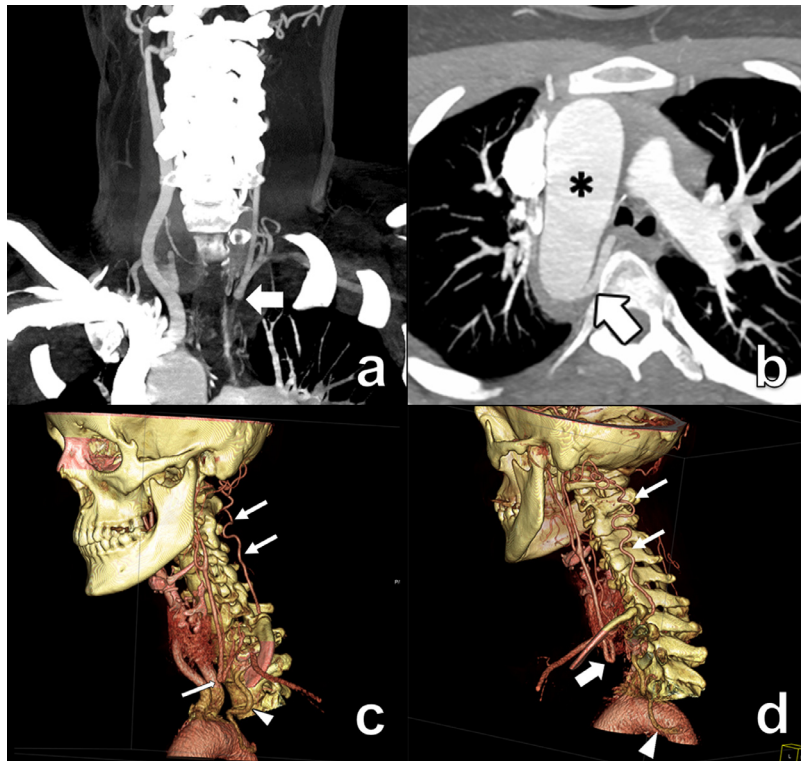


Fig. 2 – Right aortic arch with mirror image branching type and interrupted left BCA in a 35-year-old female. (a) AP—Reformatted frontal CT with angiographic reconstruction shows isolated left brachiocephalic artery (arrow). (b) Axial CT with maximum intensity projection demonstrates a right aortic arch (asterisk) with a large posterior mediastinal collateral artery (arrow) arising from its posteromedial border. (c) LAO—Left anterior oblique 3D volume rendered reformatted CT angiographic projection shows isolated left brachiocephalic artery (arrow) and large posterior mediastinal collateral artery (arrowhead) arising from the aorta. (d) LPO—Left posterior oblique 3D volume rendered reformatted CT angiographic projection shows isolated left brachiocephalic artery (arrow) and large posterior mediastinal collateral artery (arrowhead) arising from the aorta.

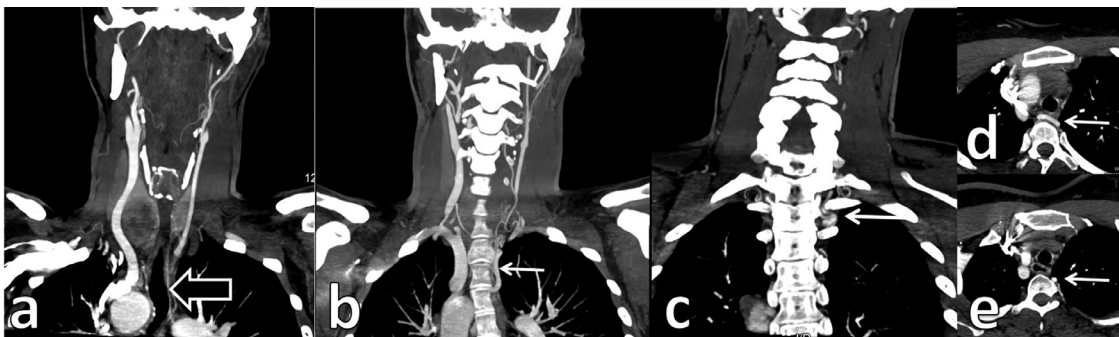


Fig. 3 – Right aortic arch with mirror image branching type and interrupted left BCA in a 35-year-old female. (a) Coronal CT with maximum intensity projection demonstrates the isolated left brachiocephalic artery with obliterated segment from aortic arch. (b) Coronal CT with maximum intensity projection demonstrates the posterior mediastinal collateral artery (arrow). (c) Coronal CT with maximum intensity projection shows the origin of the left vertebral artery (long arrow). (d and e) Axial CT with maximum intensity projection show the retroesophageal course and posterior mediastinal location of the mediastinal collateral artery (arrows).

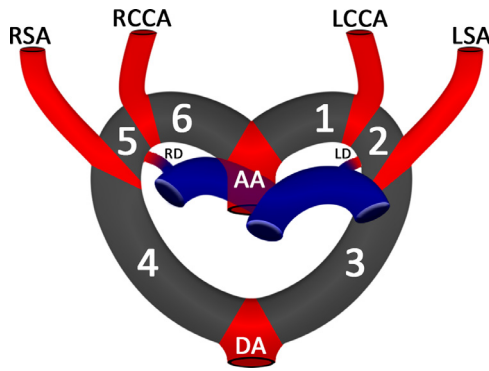


Fig. 4 – Graphic illustration for various points where regressed segments occur.

esis. Beginning at the fifth to seventh week and at subsequent times of embryogenesis the paired pharyngeal arches form and regress. The first pharyngeal arch migrates and involutes to form the maxillary artery [10]. The second pharyngeal arch forms the hyoid and stapedia arteries. The third pharyngeal arch forms the common carotid arteries and the cervical portion of the internal carotid arteries [2]. The fourth pharyngeal arch results in the aortic arch. The fifth arch typically regresses completely. Persistent fifth aortic arch is ex-

tremely rare and usually associated with cardiac anomalies, most common VSD. This anomaly results in a double lumen aortic arch ipsilateral to each other with the fourth superior to the fifth arch [9]. The sixth pharyngeal arch result in the ductus arteriosa and pulmonary arteries [2].

The aortic arch undergoes further differentiation within its ventral and dorsal components [2]. The arch regresses at a segment between the LSA and the descending aorta (DA) [2]. Abnormalities of the aortic arch occur if this regression occurs at an anomalous location or if supernumerary [2]. Right aortic arches can be classified as “mirror-image” (Fig. 5a) if the regression occurs between LSA and DA [9]. A “nonmirror-image” branching pattern occurs if this occurs between LCCA and LSA (Fig. 5b), resulting in an aberrant LSA [9]. Rarely, the left arch may disrupt between both the LCCA and LSA, as well as the LSA and descending aorta, resulting in an isolated LSA (Fig. 5c) [2]. Furthermore, if the left arch regresses between the RCCA and LCCA, and simultaneously between the LSA and DA (Fig. 5d), an exceedingly rare ILBA results [1]. In this right aortic arch variant, the order of the great vessels is: RCCA, followed by the RSA. The ILBA must receive blood flow through a left-sided patent ductus arteriosus or through recruited collateral vessels [9].

An ALSA is typically associated with nonmirror-image branching of right aortic arch, where it arises as the last vessel from the aortic arch [3]. The ALSA courses obliquely from a right caudal position, posterior to the esophagus, to

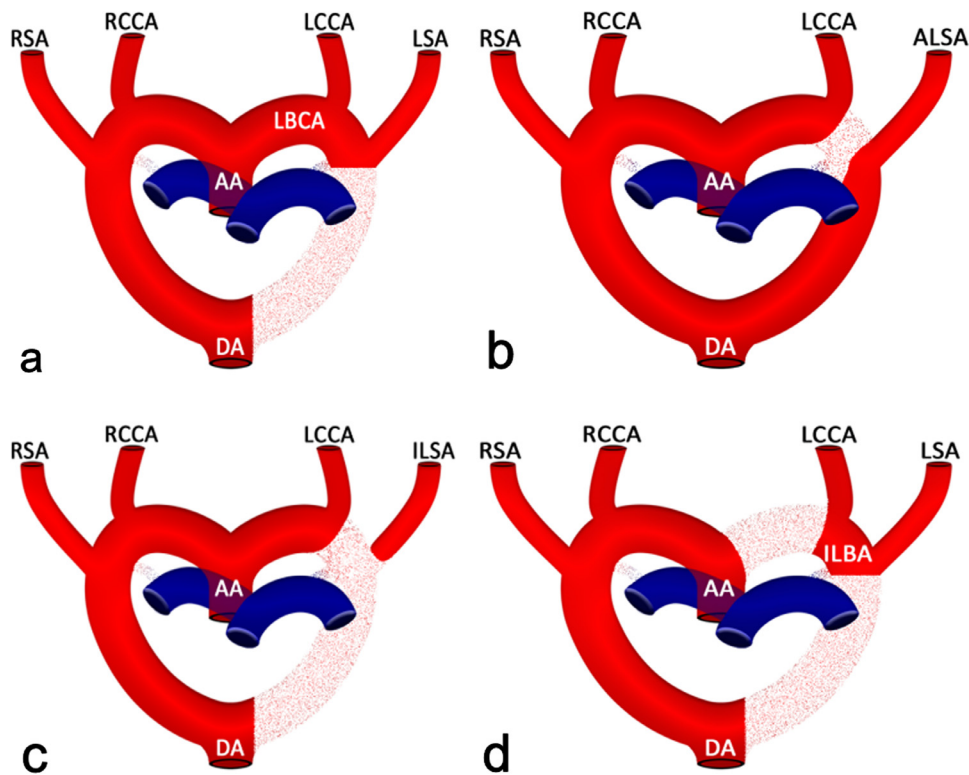


Fig. 5 – Graphic illustrations of various sites of interruption of the right sided aortic arch. (a) Right aortic arch with mirror-image branching type. (b) Right aortic arch with nonmirror-image branching and aberrant left subclavian artery. (c) Right aortic arch with isolated left subclavian artery. (d) Right aortic arch with mirror-image branching type and isolated left brachiocephalic artery. AA, ascending aorta; ALSA, aberrant left subclavian artery; DA, Descending aorta; LCCA, left common carotid artery; LSA, left subclavian artery; RCCA, right common carotid artery; RSA, right subclavian artery.

left cranial. This vessel often arises from the diverticulum of Kommerell, present in 60% of patients with this anomaly [10]. A vascular ring may form from a patent left ductus arteriosus or ligamentum arteriosum. The incidence of congenital cardiac anomaly in this group of patients is higher than the general population but still low at approximately 1%-5% [10,14].

Associated congenital cardiac anomaly occurs in 98% of mirror-image branching type of right aortic arch [8]. The most common CHD seen in adults with this branching pattern is tetralogy of Fallot [10]. The right aortic arch is usually found in 25% of tetralogy of Fallot patients and 25%-50% of truncus arteriosus although the former is much more common in adults [9]. Rarely, patients may have other anomalous great vessel branching patterns such as an isolated left subclavian artery, aberrant left brachiocephalic artery, or as in our patient, an ILBA [8].

When confronted with an adult patient with a right aortic arch on radiographs, the presence or absence of previous cardiothoracic surgery can be predictive of the great vessel branching pattern [12]. If prior surgery is evident, CHD is almost certain, and therefore the patient most likely has a “mirror-image” branching type of a right aortic arch [4]. The corollary is that, if the patient has not had evidence of surgery, they most likely do not have CHD, and therefore have a nonmirror-image branching type of right aortic arch [10].

The first case of a right aortic arch with an ILBA was described by D’Cruz and Levine et al., in 1966 [13]. Since then cases have been reported where vertebrobasilar insufficiency was clinically observed [13]. Patients with right sided aortic arch and ILBA are prone to vertebrobasilar insufficiency secondary to subclavian artery steal phenomenon [11].

In the presented case, we have observed 2 points of interruption; proximal to origin of LCCA, forming LBCA, and another cleavage just distal to ligamentum arteriosum. Retrograde filling of the most distal portion with further blood flow into LCCA and LSA have been noted from the hypertrophied posterior auricular artery—branch from external carotid artery. The hypertrophied left posterior mediastinal collateral artery, which arises directly from the right sided aortic arch, is also shown to provide supply for the left vertebral artery. In our case, there was no evidence of patent ductal arteries or steal phenomenon through pulmonary artery. The patient’s presentation of hypertension without other manifestations of vertebrobasilar insufficiency may be attributed to adequate compensatory anastomotic flow.

Multimodality imaging evaluation has been used to help detection and categorization of aortic arch abnormalities [13]. These modalities include echocardiography, computed tomography angiography, cardiac computed tomography, cardiac magnetic resonance and magnetic resonance angiography [10]. A diagnostic imaging approach should focus on elucidating the abnormal aortic arch and great vessel arrangement and determining associated cardiac, vascular or visceral congenital abnormalities. In a pediatric setting, transesophageal echocardiography is usually the optimal initial modality as it lacks ionizing radiation and contrast material administration [13].

Patient consent

Informed consent to participate in this study and for publication was obtained from the patient.

Funding

None.

Abbreviations:

AA	ascending aorta.
ALSA	aberrant left subclavian artery.
CTA	computed tomography angiography.
DA	descending aorta.
ICA	internal carotid artery.
ILBA	isolated left brachiocephalic artery.
LAO	Left anterior oblique
LARCH	left aortic arch
LBCA	left brachiocephalic artery.
LCCA	left common carotid artery.
LD	left ductus arteriosus.
LPO	Left posterior oblique.
LSA	left subclavian artery.
RARCH	right aortic arch.
RBCA	right brachiocephalic artery.
RCCA	right common carotid artery.
RD	right ductus arteriosus.
RSA	right subclavian artery.
TIA	transient ischemic attack.

REFERENCES

- [1] Malakan RE, Pouraliakbar HR. Isolation of the left brachiocephalic artery revisited: a 52-year literature review and introduction of a novel anatomic-clinical-prognostic classification. *Ann Pediatr Cardiol* 2019;12(2):117–29. doi:10.4103/apc.APC_74_1.
- [2] Priya S, Thomas R, Nagpal P, Sharma A, Steigner M. Congenital anomalies of the aortic arch. *Cardiovasc Diagn Ther* 2018;8(1):S26–44. doi:10.21037/cdt.2017.10.15.
- [3] Edwards JE. Anomalies of the derivatives of the aortic arch system. *Med Clin North Am* 1948;32:925–49. doi:10.1016/s0025-7125(16)35662-0.

- [4] Plein A, Fantin A, Ruhrberg C. Neural crest cells in cardiovascular development. *Curr Top Dev Biol* 2015;111:183–200. doi:[10.1016/bs.ctdb.2014.11.006](https://doi.org/10.1016/bs.ctdb.2014.11.006).
- [5] Stoller JZ, Epstein JA. Cardiac neural crest. *Semin Cell Dev Biol* 2005;16(6):704–15. doi:[10.1016/j.semcdb.2005.06.004](https://doi.org/10.1016/j.semcdb.2005.06.004).
- [6] Hiruma T, Nakajima Y, Nakamura H. Development of pharyngeal arch arteries in early mouse embryo. *J Anat* 2002;201(1):15–29. doi:[10.1046/j.1469-7580.2002.00071.x](https://doi.org/10.1046/j.1469-7580.2002.00071.x).
- [7] Kim BG, Kim YH, Stanley EL, Garrido-Martin EM, Lee Y J, Oh SP. CXCL12-CXCR4 signaling plays an essential role in proper patterning of aortic arch and pulmonary arteries. *Cardiovasc Res* 2017;113(13):1677–87. doi:[10.1093/cvr/cvx188](https://doi.org/10.1093/cvr/cvx188).
- [8] Morosetti D, Di Stefano C, Mondillo MT, Pensabene MC, De Corato L, Bizzaglia M, et al. Right-sided aortic arch with mirror image branching and situs solitus: a case of a 79 years old woman. *Radiol Case Rep* 2019;14(10):1246–51.
- [9] Hanneman K, Newman B, Chan F. Congenital variants and anomalies of the aortic arch. *RadioGraphics* 2017;37(1):32–51. doi:[10.1016/j.radcr.2019.07.014](https://doi.org/10.1016/j.radcr.2019.07.014).
- [10] Kanne Jeffrey P, et al. Right aortic arch and its variants. *J Cardiovasc Comput Tomogr* 2010;4(5):293–300. <https://doi.org/10.1016/j.jcct.2010.07.002>.
- [11] Potter BJ, Pinto DS. Subclavian steal syndrome. *Circulation* 2014;129(22):2320–3. doi:[10.1161/CIRCULATIONAHA.113.006653](https://doi.org/10.1161/CIRCULATIONAHA.113.006653).
- [12] Rosen RD, Bordonni B. Embryology. Aortic Arch Jan 2020 [Updated 2019 Dec 30]. In: StatPearls [Internet]. Treasure Island (FL): StatPearls Publishing <https://www.ncbi.nlm.nih.gov/books/NBK553173/>.
- [13] Mangukia C, Sethi S, Agarwal S, Mishra S, Satsangi DK. Right aortic arch with isolation of the left innominate artery in a case of double chamber right ventricle and ventricular septal defect. *Ann Pediatr Cardiol* 2014;7(2):148–51. doi:[10.4103/0974-2069.132500](https://doi.org/10.4103/0974-2069.132500).
- [14] Xu R, Shi K, Yang Z-g, Diao K-y, Zhao Q, Xu H-y, Guo Y-k. Quantified evaluation of tracheal compression in pediatric complex congenital vascular ring by computed tomography. *Sci Rep* 2018;8:11183. doi:[10.1038/s41598-018-29071-9](https://doi.org/10.1038/s41598-018-29071-9).